Neurobiology of Aging 39 (2016) 69–81

Contents lists available at ScienceDirect

Neurobiology of Aging

journal homepage: www.elsevier.com/locate/neuaging

Curcumin improves tau-induced neuronal dysfunction of nematodes

Tomohiro Miyasaka [a,*], Ce Xie [a], Satomi Yoshimura [a], Yuki Shinzaki [a], Sawako Yoshina [b], Eriko Kage-Nakadai [b,c], Shohei Mitani [b], Yasuo Ihara [a,d]

[a] Faculty of Medical and Life Sciences, Department of Neuropathology, Doshisha University, Kyotanabe-shi, Kyoto, Japan
[b] Department of Physiology, Tokyo Women's Medical University School of Medicine, Shinjuku-ku, Tokyo, Japan
[c] Advanced Research Institute for Natural Science and Technology, Osaka City University, Sumiyoshi-ku, Osaka, Japan
[d] Laboratory for Cognition and Aging, Graduate School of Brain Sciences, Doshisha University, Kizugawa-shi, Kyoto, Japan

ARTICLE INFO

Article history:
Received 7 November 2014
Received in revised form 9 November 2015
Accepted 11 November 2015
Available online 1 December 2015

Keywords:
Caenorhabditis elegans
Tau
Neurite
Neuronal dysfunction
Curcumin
Microtubules

ABSTRACT

Tau is a key protein in the pathogenesis of various neurodegenerative diseases, which are categorized as tauopathies. Because the extent of tau pathologies is closely linked to that of neuronal loss and the clinical symptoms in Alzheimer's disease, anti-tau therapeutics, if any, could be beneficial to a broad spectrum of tauopathies. To learn more about tauopathy, we developed a novel transgenic nematode (*Caenorhabditis elegans*) model that expresses either wild-type or R406W tau in all the neurons. The wild-type tau-expressing worms exhibited uncoordinated movement (Unc) and neuritic abnormalities. Tau accumulated in abnormal neurites that lost microtubules. Similar abnormalities were found in the worms that expressed low levels of R406W-tau but were not in those expressing comparative levels of wild-type tau. Biochemical studies revealed that tau is aberrantly phosphorylated but forms no detergent-insoluble aggregates. Drug screening performed in these worms identified curcumin, a major phytochemical compound in turmeric, as a compound that reduces not only Unc but also the neuritic abnormalities in both wild-type and R406W tau-expressing worms. Our observations suggest that microtubule stabilization mediates the antitoxicity effect of curcumin. Curcumin is also effective in the worms expressing tau fragment, although it does not prevent the formation of tau-fragment dimers. These data indicate that curcumin improves the tau-induced neuronal dysfunction that is independent of insoluble aggregates of tau.

1. Introduction

Alzheimer's disease (AD) is the most common cause of dementia among the elderly (Mayeux and Stern, 2012). Because of the increasing prevalence of AD with age and rapid extension of life-span, it is urgent to develop prevention and therapeutic strategies against AD (Mangialasche et al., 2010). A characteristic pathological change of AD is the formation of tau inclusions, which consist of neurofibrillary tangles and neuropil threads, in the areas of the brain where neuronal loss occurs (Braak and Braak, 1997; Gomez-Isla et al., 1997). It is believed that long-term Aβ deposition triggers the death cascade of tau, which eventually leads to neuronal death (Goate and Hardy, 2012). Several published reports using animal models have supported this amyloid cascade hypothesis (Gotz et al., 2001; Lewis et al., 2001).

Various anti-amyloid strategies have been developed, including Aβ immunization, anti–Aβ-aggregation compounds, β- or γ-secretase inhibitors, and γ-secretase modulators (Mangialasche et al., 2010). Although some of these strategies were shown to be effective in clearing the pre-existing Aβ-aggregates and preventing further Aβ deposition and its associated toxicity, clinical studies have reported that these strategies had at most limited efficacy on cognitive dysfunction of symptomatic patients (Corbett et al., 2012; Holmes et al., 2008; Selkoe, 2012). In contrast, anti-tau therapy, if any, could lead to clinical improvement in patients, as tau pathologies are closely linked to the levels of cognition in AD (Delacourte et al., 1999; Gomez-Isla et al., 1997). In addition, as the tau pathologies are associated with a number of age-related neurodegenerative diseases other than AD (Lee et al., 2001), anti-tau therapy would have beneficial effects on a broad spectrum of dementias.

The mechanisms of tau-associated neurodegeneration still remain unclear. Thus, current anti-tau strategies mostly target the aggregation of tau, which is believed to be toxic to neurons (Boutajangout et al., 2011). In fact, it is claimed that methylene blue,

* Corresponding author at: Faculty of Life and Medical Sciences, Department of Neuropathology, Doshisha University, 1-3 Tatara-Miyakodani, Kyotanabe-shi, Kyoto, 610-0394, Japan. Tel.: +81 774 65 6137; fax: +81 774 65 6135.
E-mail address: tomiyasa@mail.doshisha.ac.jp (T. Miyasaka).

0197-4580/
http://dx.doi.org/10.1016/j.neurobiolaging.2015.11.004

a potent tau-aggregation inhibitor, prevented the progression of clinical symptoms (Wischik and Staff, 2009). However, it is not yet known if aggregation or inclusion formation of tau is responsible for the pathogenesis of tauopathies.

One way to efficiently screen for drugs is to test naturally occurring compounds that have been validated epidemiologically. Curcumin, a yellow phytochemical in the rhizome of *Curcuma longa*, which has various biological effects (Belkacemi et al., 2011), has been used as a spice in India. Epidemiological studies reported that the prevalence of AD in India is less than that in the US, which may suggest that a curcumin-rich diet might decrease the risk of developing AD (Chandra et al., 2001). We thus hypothesized that curcumin may attenuate tau-induced neurodegeneration.

In this study, we developed several *Caenorhabditis elegans* models of tauopathy in which the neurons express human tau. We observed tau-dependent neuronal dysfunction and morphological abnormalities even in the absence of insoluble tau-aggregates. Furthermore, curcumin is effective in treating the tau-induced neuronal dysfunction.

2. Materials and methods

2.1. Development and maintenance of worm strains

Human tau, tau fragment, or DsRed complementary DNA (cDNA) was subcloned downstream of the "pan-neuronal" unc-119 promoter (Punc-119) sequence in the pFXneo-punc119 vector. For the Punc-119-driven DsRed transgenic (Tg) worms, the expression vector was diluted with the pBluescript vector and injected into wild-type worm, N2. For the Punc-119-driven tau-Tg worms, the vectors were coinjected into N2 with the marker pFX-Pges-1:enhanced green fluorescent protein. Germline transformation and generation of genome-integrated Tg lines were performed using ultraviolet irradiation, as described previously (Mello and Fire, 1995; Mello et al., 1991; Mitani, 1995). The dose of radiation for DNA integration was 250 J/m^2 or 300 J/m^2. The integrated Tg lines were backcrossed to N2 5 (for tau) or 2 (for DsRed) times before analysis. The Tg nematodes contained multiple copies of the transgene. The Tg strains used are as follows; Mock-Tg (tmIs388), WT4R-Tg (tmIs389 and tmIs390), WT3R-Tg (tmIs252), P301L-Tg (tmIs227), R406W-Tg (tmIs226), 4R-tau C-terminal fragment-Tg (CT4R, tmIs712), and DsRed-Tg (tmIs591) (Xie et al., 2014). For morphological studies, the following tau-Tg lines that were crossbred with the DsRed-Tg line were used: Mock/DsRed-Tg (tmIs388/591), WT4R/DsRed-Tg (tmIs390/591), and R406W/DsRed-Tg (tmIs226/591). All the *C. elegans* strains were maintained on the nematode growth medium (NGM)-containing plates that were spread with *Escherichia coli* OP50 under standard conditions according to Brenner with modifications by Way and Chalfie (Brenner, 1974; Way and Chalfie, 1988).

2.2. Behavioral analyses

Healthy adult worms were transferred to a new NGM plate to lay eggs. Parent worms were picked off the plate 2 hours later, and the resulting synchronized eggs were cultivated at 20 °C until isolation. For isolation, worms at varying stages were selected individually and placed on new 3.5-cm plates. For the estimation of uncoordinated movement (Unc), worms were observed under a microscope. The severity of Unc was scored as follows: normal, wide bending with fast movement; Unc, narrow bending with slow movement; severe Unc, narrow bending with slower or negligible movement. Liquid thrashing assays were performed as previously described with minor modifications (Kraemer et al., 2003). The worms were placed in a drop of M9 buffer (22-mM KH_2PO_4, 42-mM Na_2HPO_4, 85-mM NaCl, 1-mM $MgSO_4$) on a glass slide, and the thrashing movements were counted for 30 seconds under a microscope. All the assays were performed blindly. Twenty worms were used in each assay for each experiment, and the experiment was performed independently 3 to 4 times. Thus, 60 to 80 worms were assessed for each line. The touch assay was performed as described previously (Miyasaka et al., 2005a). The number of responses to 10 touch trials, 5 for the anterior and 5 for the posterior, were counted.

2.3. Biochemical analyses

Synchronized worms were harvested in M9 buffer and pelleted by brief centrifugation. After washing with M9 buffer, the worm pellets were weighed and stored at −80 °C. For the preparation of the total worm lysates, the pellets were sonicated in the sodium dodecyl sulfate (SDS) sample buffer (80-mM Tris-HCl, 2% SDS, 10% glycerol, 1% 2-mercaptoethanol, pH 6.8) and cleared by ultracentrifugation at 150,000× *g* for 10 minutes at 20 °C. The SDS-soluble fractions were used for Western blot analysis as described previously (Miyasaka et al., 2005b). The protein concentration for each sample was normalized by Coomassie Brilliant Blue (Wako Pure Chemical Industries, Ltd, Osaka, Japan) staining on SDS-polyacrylamide gel electrophoresis gels. The detergent solubility of tau was analyzed by sequential solubilization as described previously with minor modifications (Kraemer et al., 2003). Briefly, worm pellets were homogenized using a glass-teflon homogenizer in high salt re-assembly buffer (RAB) (0.1-M 2-Morpholinoethanesulfonic acid, 0.5-mM MgSO4, 1-mM EGTA, 0.5-M NaCl, pH 6.8) supplemented with protease and phosphatase inhibitors followed by centrifugation at 3000× *g* for 3 minutes to remove the unhomogenized worms (Hasegawa et al., 1992; Miyasaka et al., 2005b). The resulting supernatants were further centrifuged at 150,000× *g* for 20 minutes, and the pellets were homogenized in radioimmunoprecipitation assay (RIPA) buffer (50-mM Tris, 150-mM NaCl, 1% NP-40, 0.5% deoxycholate, 0.1% SDS, pH 8.0) and centrifuged at 150,000× *g* for 20 minutes. The residual RIPA-insoluble pellets were sonicated in the SDS sample buffer (RIPA-insoluble fraction). The aliquots from the RAB- and RIPA-soluble supernatants were mixed with the SDS sample buffer and used for Western blot analysis. The microtubules and free tubulin were prepared as described previously (Miyasaka et al., 2010). Briefly, freshly harvested worms were homogenized in a buffer containing taxol and Guanosine triphosphate and subjected to ultracentrifugation. The supernatants and pellets, which consisted of free tubulin and microtubule fractions, respectively, were analyzed by Western blotting. For the absolute quantification, worm tubulin and recombinant human tau (4-repeat 383-amino acid isoform) were purified as described previously (Aamodt and Culotti, 1986; Aoyagi et al., 2007).

2.4. Morphological analyses

For the morphological study, the tau/DsRed-Tg worms were placed into a drop of M9 buffer containing 50-mM NaN_3 on agar pads and covered with a cover glass. For immunocytochemical analysis, synchronized worms at various ages were harvested and kept in 4% paraformaldehyde at 4 °C for 24 hours. The fixed worms were dehydrated with 100% ethanol, immersed in 100% xylene, and embedded in a paraffin block. Paraffin-embedded sections at a 6-μm thickness were processed using a microtome and placed onto MAS-coated glass slides (Matsunami Glass Ind, Ltd, Osaka, Japan). Deparaffinized and hydrated sections were dipped into the target retrieval solution (DAKO, Glostrup, Denmark) at 95 °C for 15 minutes and then blocked with 5% bovine serum albumin in tris-buffered saline (TS; 50-mM tris-HCl, 150-mM NaCl, pH 7.6). The

specimens were incubated for 16–24 hours with primary antibodies in 1% bovine serum albumin in TS. After washing with TS, the bound antibodies were visualized using Alexa-conjugated secondary antibodies (Molecular Probes, Inc, Eugene, OR, USA). The specimens were mounted with VECTASHIELD (Vector Laboratories, Inc, Burlingame, CA, USA) and observed under a Zeiss Axioskop microscope equipped with the Lasersharp2000 software (Carl Zeiss Inc, Thornwood, NY, USA).

2.5. Drug treatment

The chemical compounds were dissolved in the appropriate solvents and stored at −20 °C. For the drug administration, the compounds were diluted in M9 buffer and directly spread onto an NGM plate. The worms were synchronized and grown on the drug-containing plates for 4 days and then analyzed. The sensitivities of the worms to aldicarb and levamisole were assessed by the procedure described previously (Kraemer et al., 2003).

2.6. Antibodies and compounds

Anti-tauN and anti–UNC-119N antibodies were raised against the synthetic peptides AEPRQEFEVMEDHAGGC and QQSIAPGSATFPSQMPRGGC, respectively. These peptides were conjugated to Keyhole limpet hemocyanin. The specific IgG was affinitypurified using antigenic peptides that were conjugated to activated thiol-Sepharose 4B (GE healthcare Bio-Science KK, Tokyo, Japan) according to the manufacturer's instruction. Other antibodies used in this study were pool-2 (anti–pan-tau, a generous gift from Dr. Mori), DM1A (anti–α-tubulin, Sigma-Aldrich, St. Louis, MO, USA), 1A4 (anti–α-actin, Sigma), 6–11B1 (anti–acetylated α-tubulin, Sigma), 6C5 (anti-GAPDH, Abcam, Cambridge, MA, USA), tau-1 (anti-dephosphoSer199 and dephosphoSer202 tau, Chemicon, Temecula, CA, USA), AT8 (anti-phosphoSer202 and phosphoSer205 tau, Innogenetics, Zwijndrecht, Belgium), AT100 (anti–phosphoThr212 and phosphoSer214 tau, Innogenetics), pS262 (anti-phosphoSer262 tau, Invitrogen), paired helical filaments (PHF)-1 (anti-phosphoSer396 and phospho404 tau, a generous gift from Dr. Davies), MC-1 (conformation-dependent anti-tau, from Dr. Davies), and anti-DsRed monoclonal and polyclonal antibodies (Clontech laboratories Inc, Mountain View, CA, USA). Other compounds used in this study were purchased from Nacalai tesque, Inc (Kyoto, Japan).

3. Results

3.1. The generation of tau-transgenic worms

We previously reported that *C. elegans* is a useful tool for studying neurodegenerative diseases, especially tauopathy. Using the mec-7 promoter, we found that tau causes behavioral and morphological abnormalities in the mechanosensory neurons. The accumulation of tau, which is associated with neuritic abnormalities, is preceded by the neuronal dysfunction (decreased touch sensitivity) (Miyasaka et al., 2005a). This model system was useful to correlate morphological abnormalities with neuronal functions, but it was unsuitable for biochemical analysis. Thus, we generated worm lines that expressed human tau in all the neurons that were under the control of the unc-119 promoter (Fig. 1A; Maduro and Pilgrim, 1995). We first analyzed the expression pattern of tau using paraffin-embedded sections by immunocytochemistry. Tau was present in the neurons in the nerve ring, ventral nerve cord, dorsal nerve cord, lumbar ganglia, and thin neurites throughout the body, but the expression levels of tau in the individual neurons appeared to vary (Fig. 1B). This pan-neuronal expression pattern was similar to the one that was previously reported (Maduro and Pilgrim, 1995). To verify the expression of tau in each line, Western blot analysis was performed on the total lysates of adult worms on the fourth day after hatching. As shown in Fig. 1C, tmIs389 and tmIs390 expressed low and high levels of the wild-type 4-repeat tau, respectively. The amount of tau expressed in tmIs390 was approximately 3 times higher than the levels in tmIs389. Similarly, the expression levels of wild-type tau in tmIs252 were 4 times higher than the levels in tmIs389. There were comparable levels of R406W tau in tmIs226 and wild-tau in tmIs389, and tmIs227 expressed P301L tau 7 times more than wild-type tau in tmIs389 (Fig. 1C and D). The expression levels of tubulin and glyceraldehyde-3-phosphate dehydrogenase did not significantly differ between the lines (Fig. 1C and D). Because there is an extra 23 amino acids at the N-terminus of tau that was derived from the 5′-terminal sequence of unc-119, an anti–unc-119N antibody was raised against the synthetic peptide corresponding to amino acids 7–23 of unc-119. This antibody was used to label the proteins expressed in our system. Using this antibody, we found that the tau expression levels in all the lines used in this study were 3 to 5 times lower than the expression levels of enhanced green fluorescent protein in tmIs522 or DsRed in tmIs591, which are the lines that showed no growth or behavioral abnormalities (data not shown). The expression levels of tau depended on the copy number of the vectors inserted into the genome of the worm (data not shown). However, there was no inhibition of unc-119 expression in any of the lines used in this study. These results indicate that the abnormalities in the tau-Tg worms were not caused by overexpression of nonspecific proteins and the integration of the excess copies of unc-119 promoter. These lines will be referred to as follows: Mock-Tg (tmIs388), WT4R(L)-Tg (tmIs389), WT4R(H)-Tg (tmIs390), WT3R(H)-Tg (tmIs252), R406W(L)-Tg (tmIs226), and P301L(H)-Tg (tmIs227).

3.2. Behavioral abnormality of tau-expressing worms

We did not observe premature mortality during development in any of the Tg lines. However, behavioral abnormalities were present in the WT4R(H)-Tg, WT3R(H)-Tg, R406W(L)-Tg, and P301L(H)-Tg lines. The slower-moving worms left traces on the plate that were narrower than the waves generated by the Mock-Tg or WT4R(L)-Tg worms, although the severity varied among the individual worms. The number of worms that were severely affected with the Unc phenotype was the highest in the WT4R(H)-Tg and P301L(H)-Tg lines and moderate in the WT3R(H)-Tg and R406W(L)-Tg lines (Fig. 2A). These abnormalities appeared on the second day after hatching (data not shown). We quantified the Unc phenotype by the frequency of thrashing in a droplet of buffer (Fig. 2B). This liquid thrashing analysis indicated that the frequency of thrashing in the WT4R(H)-Tg, R406W-Tg(L), and P301L-Tg(H) lines was significantly lower than the frequencies in the Mock-Tg or WT4R(L)-Tg lines on the second day after hatching. These abnormalities worsened on the fifth day after hatching. There was a significant increase in the frequency of thrashing in the WT3R(H) line on the second day after hatching. The frequency of thrashing did not decrease in the Mock-Tg and WT4R(L)-Tg lines throughout the experiment. Taken together, we conclude that tau expression causes neuronal dysfunction in the worms in a dose-dependent manner. Furthermore, by comparison with WT4R(L)-Tg line, the frontotemporal dementia with parkinsonism-17 tau mutant (R406W) appeared to enhance tau-induced neuronal dysfunction. The affected lines exhibited a slight "dumpy" morphology resembling the unc-119 mutant strain (data not shown). In our *C. elegans* model, the behavioral phenotype caused by the 3-repeat tau was not as severe as the 4-repeat tau. In these lines, the 3-repeat and 4-repeat tau proteins had comparable expression levels. The mean life spans of the affected lines were slightly but significantly shorter than the life

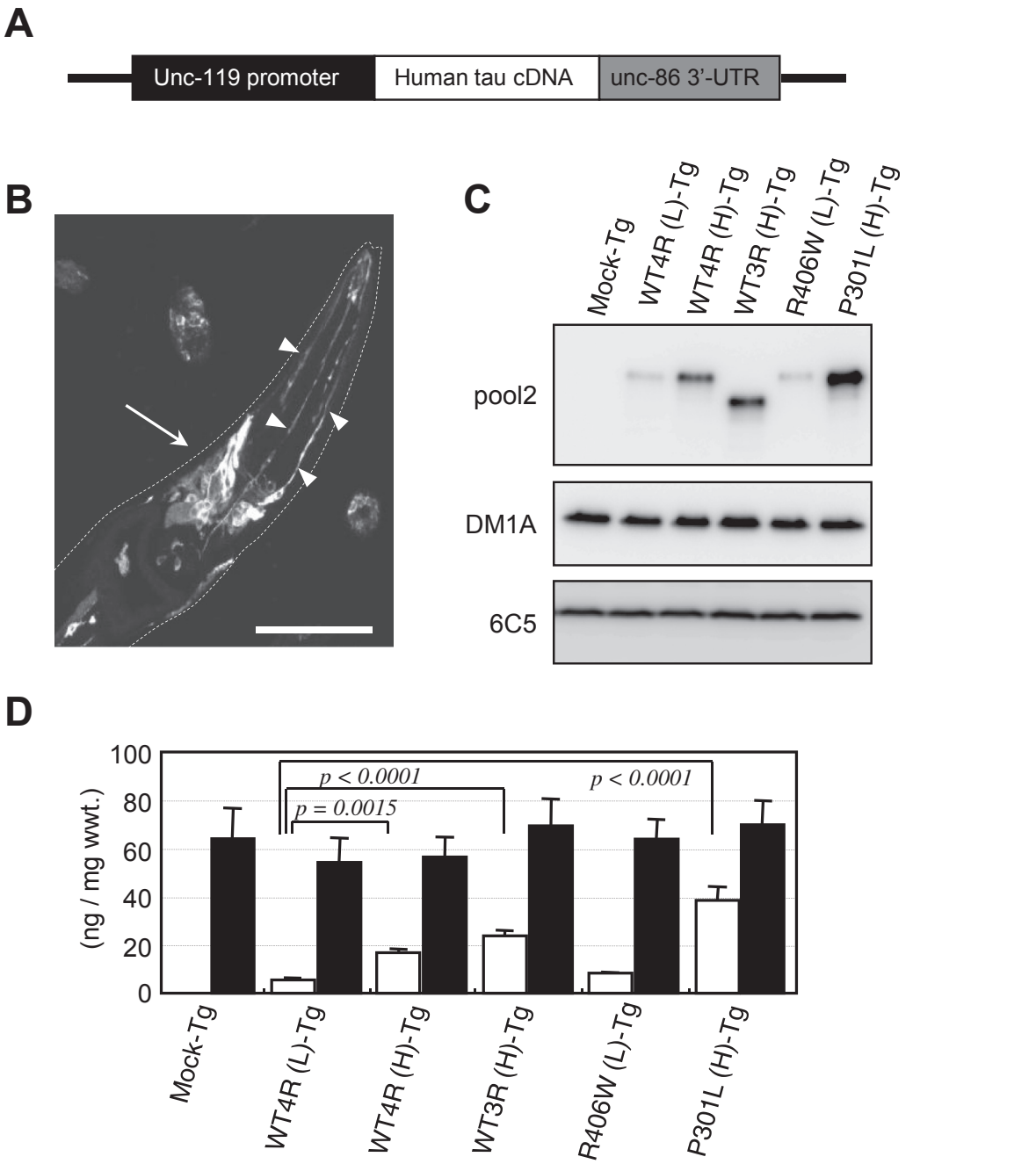

Fig. 1. Pan-neuronal tau expression in *Caenorhabditis elegans* causes uncoordination. (A) Human tau cDNA encoding wild-type 0N4R (WT4R), wild-type 0N3R (WT3R), R406W mutant 0N4R (R406W), or P301L mutant 0N4R (P301L) was expressed under the control of unc-119 promoter, which resulted in pan-neuronal expression in *C. elegans*. (B) Immunocytolabeling of tau using pool2 revealed the expression of human tau in the cell body (arrow) and neurites (arrowheads) around the nerve ring and other neurons, including the ventral nerve cord, dorsal nerve cord, and lumbar ganglia (not shown). The body wall is outlined by a dashed line. (C) Equal amounts of the total lysate from each worm line were subjected to Western blotting using the anti-tau (pool2), anti–α-tubulin (DM1A), and anti-GAPDH (6C5) antibodies. (D) The expression levels of tau (open bar; pool2) and α-tubulin (closed bar; DM1A) are shown. The data represent the means ± standard error of the protein amount in the worm pellet. Statistical significance was evaluated using a 2-way ANOVA followed by the Tukey/Kramer post hoc test. Abbreviations: ANOVA, analysis of variance; GAPDH, glyceraldehyde-3-phosphate dehydrogenase.

spans of the healthy lines (Supplementary Fig. 1). Because tau expression and the phenotype in the P301L(H)-Tg line were unstable with passage, we used the Mock-Tg, WT4R(L)-Tg, WT4R(H)-Tg, and R406W(L)-Tg lines for the further morphological and pharmacological studies.

3.3. Biochemical characteristics of the tau expressed in worms

Tauopathy is defined by the neurodegeneration associated with intraneuronal aggregation of abnormally phosphorylated tau. Several animal models fulfilled these criteria. However, recent findings questioned whether these biochemical abnormalities of tau are required for neurodegeneration (Berger et al., 2007; Maeda et al., 2006, 2007; Miyasaka et al., 2005a; Sahara et al., 2008; Santacruz et al., 2005). Total lysates from the Mock-Tg and tau-Tg lines were subjected to Western blotting using anti–phospho-tau-specific or anti–dephospho-tau-specific antibodies. As shown in Fig. 3A, all antiphospho-tau antibody used here labeled the tau expressed in the worms. This finding indicates that exogenously expressed tau even in the healthy WT4R(L)-Tg worms is highly

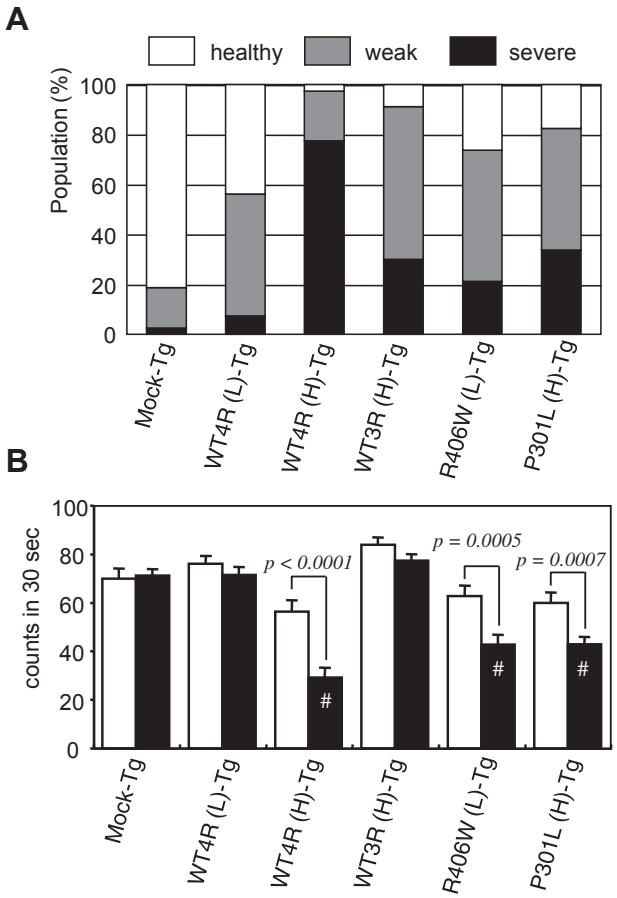

Fig. 2. Behavioral abnormalities of tau-Tg worms. (A) The numbers of healthy (white), weak Unc (gray), and severe Unc (black) worms were counted on the fifth day after hatching as described in Section 2. The percent of the population for each phenotype is given. (B) Thrashing in buffer for 30 sec for the indicated worms on the second (white bar) and fifth (black bar) day after hatching was counted. The data indicate the means ± standard error (n = 56–60). The statistical significance compared with Mock-Tg was analyzed using the Tukey/Kramer test ($^{\#}p < 0.01$), and the indicated pairs were analyzed using Student *t* test. Abbreviations: Tg, transgenic; Unc, uncoordinated movement.

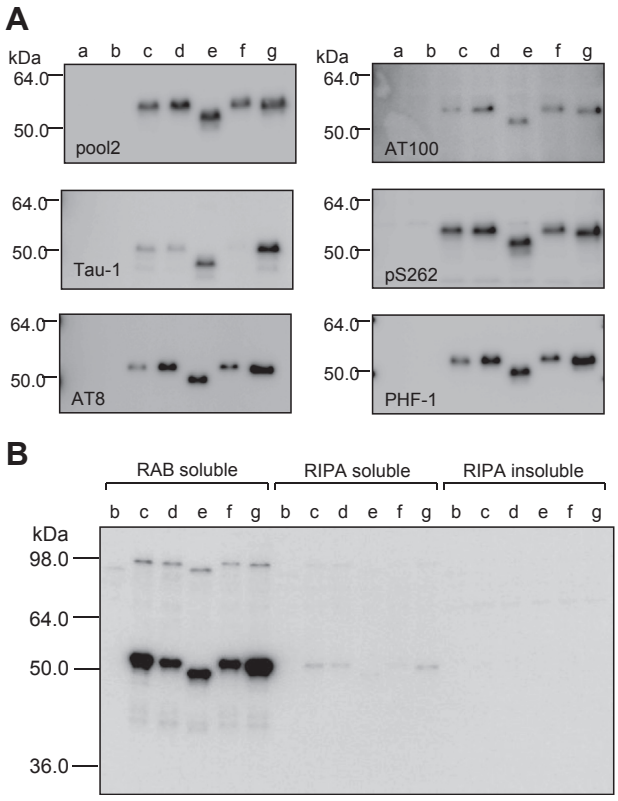

Fig. 3. Biochemical properties of tau in pan-neuronal tau-Tg worms. (A) The total lysate from N2 (a), Mock-Tg (b), WT4R(L)-Tg (c), WT4R(H)-Tg (d), WT3R(H)-Tg (e), R406W-Tg (f), or P301L-Tg (g) on the fifth day after hatching was subjected to Western blotting using phosphorylation-dependent and -independent anti-tau antibodies as indicated. The serine and threonine residues examined here were phosphorylated to similar extents. (B) RAB-soluble, RIPA-soluble, and RIPA-insoluble/SDS-soluble fractions were subjected to Western blotting using the pool2 antibody. The RIPA-insoluble tau was undetectable in each line even on the 18th day after hatching. Abbreviations: RAB, re-assembly buffer; RIPA, radioimmunoprecipitation assay; SDS, sodium dodecyl sulfate; Tg, transgenic.

phosphorylated, and the phosphorylation is to a similar extent found in PHF-tau. We next determined whether detergent-insoluble tau accumulated in these lines. The lysates were sequentially solubilized with RAB, RIPA, and SDS sample buffer. Western blot analysis indicated that tau is soluble in our models on the 10th day after hatching (data not shown) as well as the 18th day after hatching, which is nearly at the end of the worm lifespan (Fig. 3B). Dot blotting with MC-1 did not label tau in these worms (data not shown). Thus, we conclude that in our worm models, tau is phosphorylated to a high extent, but it does not form any insoluble aggregates.

3.4. Morphological abnormalities in the neuron of the tau-Tg worms

We previously demonstrated that functionally affected, tau-expressing mechanosensory neurons displayed neuritic abnormalities but not neuronal death (Miyasaka et al., 2005a). To explore the morphological abnormalities in the neurons affected by tau expression, the Mock-Tg and tau-Tg lines, including WT4R(L)-Tg, WT4R(H)-Tg, and R406W(L)-Tg, were crossbred with the line expressing DsRed in all the neurons (tmIs951). Although the behavioral abnormalities seemed to be slightly more advanced in the tau-Tg lines, the overall extent of severity was not altered in the crossbred tau-Tg lines regardless of the presence of DsRed (data not shown). The Mock/DsRed-Tg lines displayed no morphological abnormalities compared with the DsRed-Tg lines (Fig. 4A). However, in the behaviorally affected worms, WT4R(H)/DsRed-Tg and R406W(L)/DsRed-Tg, 2 thin neurites running along the body axis in the caudal half showed abnormal morphologies, including kinks and protrusions (Fig. 4C–E). Although the population was small, similar neurites were observed in the aged WT4R(L)/DsRed-Tg worms (Fig. 4B and E). One of the 2 neurites affected was identified as ALN due to its localization relative to the cell body. Although the other neurites were unable to be identified, immunocytochemical analysis indicated that this neurite seemed to follow the course of PLM, which can be labeled by the 6–11B1 antibody. In rare cases, transversely oriented neurites running into protrusions were found (data not shown). Although the precise origin of the protrusions is unknown, it is possible that those are abnormally enlarged spines. These morphological abnormalities of neurites resemble the abnormalities found in aged worms (Tank et al., 2011; Toth et al., 2012). The population of WT4R(L)/DsRed-Tg worms that had kink neurites and protrusions was small but significantly larger than that population of the Mock/DsRed-Tg lines and gradually became larger with age (Fig. 4G). The number of kink neurites was larger in the behaviorally affected lines on the fifth day after hatching and continued to exist throughout life (Figs. 2 and 4G). In the R406W(L)-Tg lines, the population of the worms that had kink

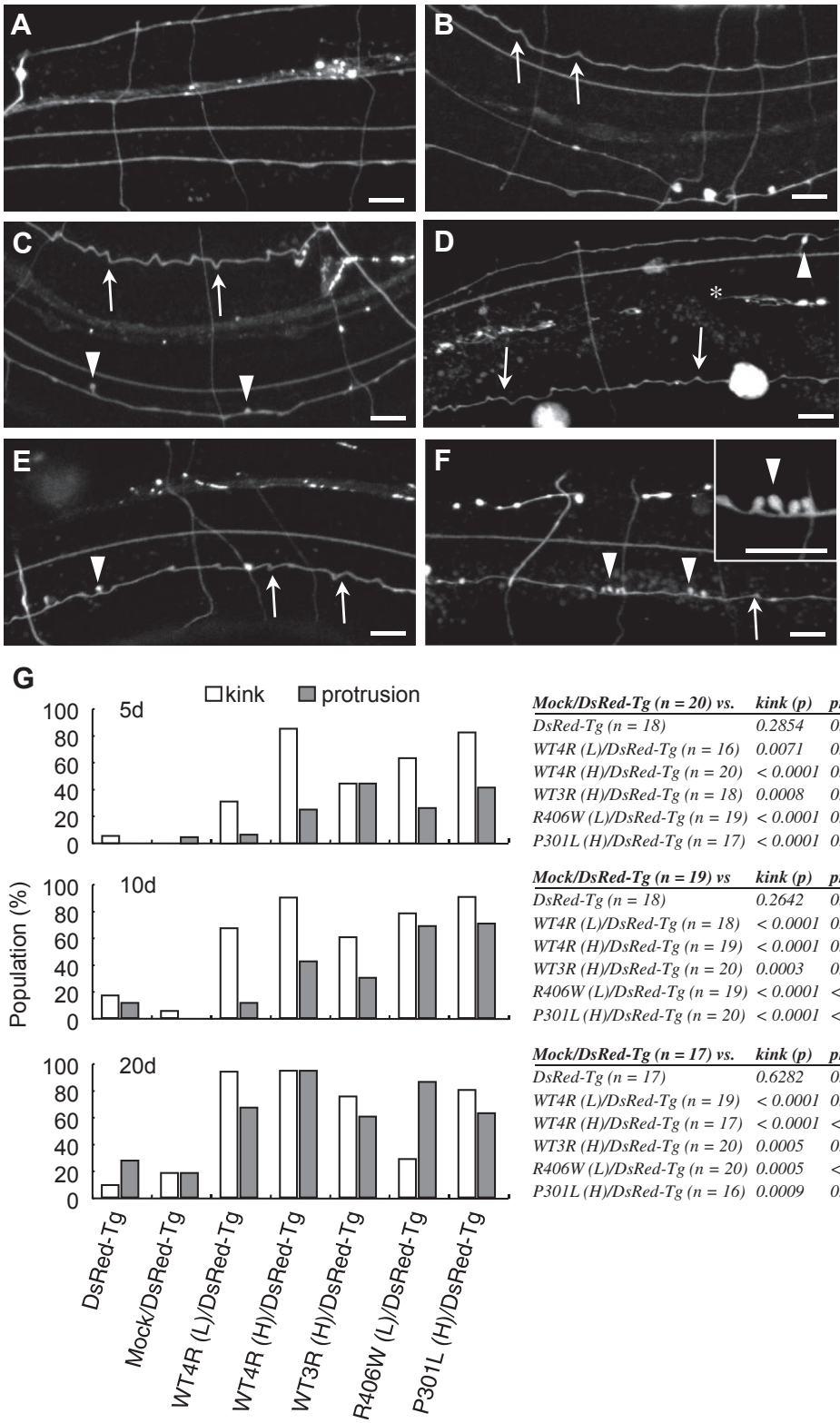

Mock/DsRed-Tg (n = 20) vs.	*kink (p)*	*protrusion (p)*
DsRed-Tg (n = 18)	*0.2854*	*0.3363*
WT4R (L)/DsRed-Tg (n = 16)	*0.0071*	*0.8708*
WT4R (H)/DsRed-Tg (n = 20)	*< 0.0001*	*0.0765*
WT3R (H)/DsRed-Tg (n = 18)	*0.0008*	*0.0043*
R406W (L)/DsRed-Tg (n = 19)	*< 0.0001*	*0.0652*
P301L (H)/DsRed-Tg (n = 17)	*< 0.0001*	*0.0077*

Mock/DsRed-Tg (n = 19) vs	*kink (p)*	*protrusion (p)*
DsRed-Tg (n = 18)	*0.2642*	*0.1352*
WT4R (L)/DsRed-Tg (n = 18)	*< 0.0001*	*0.1352*
WT4R (H)/DsRed-Tg (n = 19)	*< 0.0001*	*0.0015*
WT3R (H)/DsRed-Tg (n = 20)	*0.0003*	*0.0094*
R406W (L)/DsRed-Tg (n = 19)	*< 0.0001*	*<0 .0001*
P301L (H)/DsRed-Tg (n = 20)	*< 0.0001*	*< 0.0001*

Mock/DsRed-Tg (n = 17) vs.	*kink (p)*	*protrusion (p)*
DsRed-Tg (n = 17)	*0.6282*	*0.6715*
WT4R (L)/DsRed-Tg (n = 19)	*< 0.0001*	*0.0057*
WT4R (H)/DsRed-Tg (n = 17)	*< 0.0001*	*< 0.0001*
WT3R (H)/DsRed-Tg (n = 20)	*0.0005*	*0.0089*
R406W (L)/DsRed-Tg (n = 20)	*0.0005*	*< 0.0001*
P301L (H)/DsRed-Tg (n = 16)	*0.0009*	*0.0084*

Fig. 4. Age-dependent neuritic abnormalities in the tau-expressing worms. (A–F) CLSM images of thin neurites in the posterior part of the body are shown. Mock/DsRed-Tg (A), WT4R(L)/DsRed-Tg (B and F), WT4R(H)/DsRed-Tg (C), R406W(L)/DsRed-Tg (D), and P301L(H)/DsRed-Tg (E) were observed under CLSM on the fifth day (not shown), 10th day (A–E), and 20th day (F) after hatching. Abnormal kinks (arrows) and protrusions (arrowheads) are indicated. Bars = 10 μm. (G) The populations of the affected worms were quantified. Statistical analysis was performed using the chi-squared test for independence compared to non–tau-Tg lines. Abbreviations: CLSM, confocal laser scanning microscopy; Tg, transgenic.

neurites decreased on the 20th day after hatching. This may be caused by a loss of degenerating neurites (data not shown). The frequencies of protrusions were moderate in the tau-Tg lines on the fifth day after hatching, but they significantly increased with age (Fig. 4G). Prospective observations of individual worms indicated that the affected neurites gained more kinks and formed more

protrusions until finally fragmentation occurred (data not shown). Thus, the abnormal neurites in the tau-expressing worms likely represent progressive neuronal degeneration.

3.5. Tau accumulation in the affected neurites

To determine whether tau accumulates in the affected neurites, immunocytochemistry was performed on the paraffin-embedded sections of the worms. As the DsRed fluorescence was lost by the paraffin-embedding process, whole neuronal morphology was visualized with anti-DsRed antibodies. Double immunostaining for tau and DsRed indicated that the relative amount of tau was higher in the affected neurites than in the normal neurites (Fig. 5). Furthermore, tau was concentrated at the turning point of the kink neurites and protrusions (arrow and arrowheads in Fig. 5), but there were no neurofibrillary tangle-like inclusions. Thus, the morphological abnormalities in the neurites of the tau-Tg worms were associated with tau accumulation.

3.6. Affected neurites are depleted of tubulin

Tauopathy-affected neurons were known to be devoid of microtubules or tubulin. This characteristic is conserved across various animal models of tauopathy, including *C. elegans* (Miyasaka et al., 2005a; Tatebayashi et al., 2002). We examined the levels of tubulin in the neurites with tau accumulation. As shown in Fig. 6, the affected thin neurites had less tubulin than did the intact neurites. Furthermore, at the turning points of the kinks and protrusions, the tubulin-stained area was thinner than in the other portions of the affected neurites. Co-immunolabeling with tau and tubulin clearly showed an inverse correlation between neurites that had high and low tau expression (Fig. 6J–L). Together with the results in Fig. 5, it is possible that the amounts of tau and tubulin may determine the fate of the neurons.

3.7. The effects of small chemical compounds on neuritic abnormalities in the tau-Tg worms

The development of anti-tauopathy drugs is a major issue to be studied. Chemical compounds were rigorously screened for their potential to inhibit tau aggregation, and some compounds were reported to improve tauopathy (Wischik and Staff, 2009). Although many investigators have been involved in the screening for these antiaggregation compounds, we cannot exclude the possibility that compounds that do not have antiaggregation properties may improve tauopathy. The *C. elegans* model of tauopathy is useful for such chemical screenings because of the easy application of compounds and expansion of scale, as well as rapid evaluation of neuronal function. Curcumin is a yellow-colored chemical compound purified from the root of *C. longa*, a turmeric spice. In vitro and in vivo studies indicate that curcumin prevented Aβ aggregation and reduced the extent of Aβ deposition and cognitive dysfunction of APP (amyloid precursor protein)-Tg mice (Begum et al., 2008; Lim et al., 2001; Ma et al., 2009; Ono et al., 2004; Yang et al., 2005). Curcumin has a wide variety of biological effects, including antioxidant, anti-inflammatory, and anticancer activities (Belkacemi et al., 2011). The antagonizing effects of curcumin on Aβ aggregation could account for its beneficial effects on APP-Tg animals. However, it is possible that other functions of curcumin may be responsible for the protection against AD.

The tau-Tg worms were grown on a plate supplemented with curcumin and analyzed their behavior. As shown in Fig. 7A and B, the WT4R(H)-Tg lines showed a severe Unc phenotype on plates containing either the vehicle or low-dose (10 μg/plate; 3 μM) curcumin. However, high doses (100 μg/plate; 30 μM) of curcumin significantly reduced the proportion of severely affected worms compared with the vehicle-treated worms. Curcumin was also effective in treating the behavioral abnormalities and the low liquid thrashing in the mutant tau-expressing worms (Fig. 7B and Supplementary Fig. 2). Curcumin treatment did not affect the expression of tau, but it did slightly reduce the expression of α-tubulin (Fig. 8 and data not shown). Similarly, curcumin treatment did not affect tau phosphorylation (Fig. 8). The curcumin-treated worms were slightly smaller than the vehicle-treated worms (data not shown). Thus, curcumin suppressed neuronal dysfunction by inhibiting the mechanisms downstream of a pivotal step shared by the wild-type and mutant tau. We further analyzed other previously reported compounds, such as methylene blue, resveratrol, and trehalose (Tanaka et al., 2004; Wang et al., 2006; Wischik et al., 1996). High doses (200 μM) of methylene blue ameliorated the behavioral abnormalities in the tau-expressing worms. However, the other compounds did not improve neuronal dysfunction in the Tg worms (data not shown).

3.8. Curcumin improved neuritic abnormalities in the tau-Tg worms

We further examined the effects of curcumin on morphological abnormalities in the tau-Tg worms. To quantify these abnormalities, we counted the kinks and protrusions along a 200-μm length of the neurites in the caudal half. This length spans most of the highlighted neurites. As shown in Fig. 9, curcumin significantly reduced the number of kinks in the affected neurites in both the WT4R(H)-

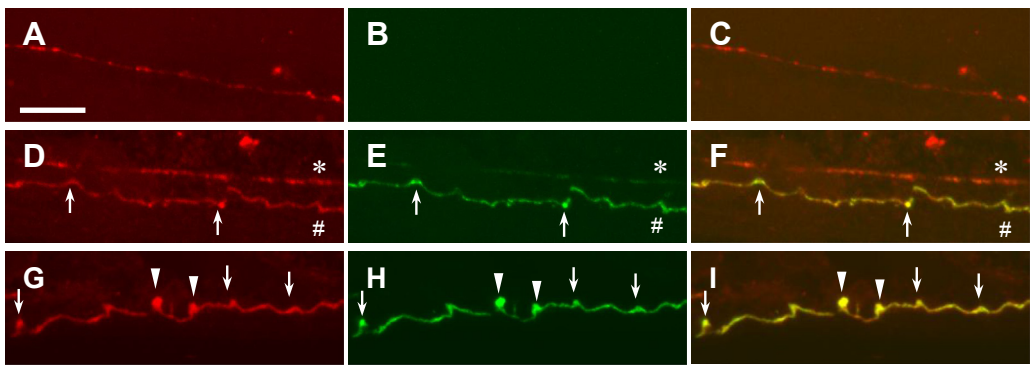

Fig. 5. The localization of tau in the affected neurites. Paraffin-embedded sections of Mock-Tg (A–C) and R406W(L)-Tg worms (D–I) were colabeled with anti-DsRed monoclonal (A, D, and G) and pool2 (pan-tau) (B, E, and H) antibodies. The merged view is also shown (C, F, and I). Tau was more intensely labeled in the affected neurites (#) compared to the normal neurites (*). Tau was located in the abnormal swelling portions associated with kinks (arrows) and protrusions (arrowheads). Bar = 10 μm. Abbreviation: Tg, transgenic.

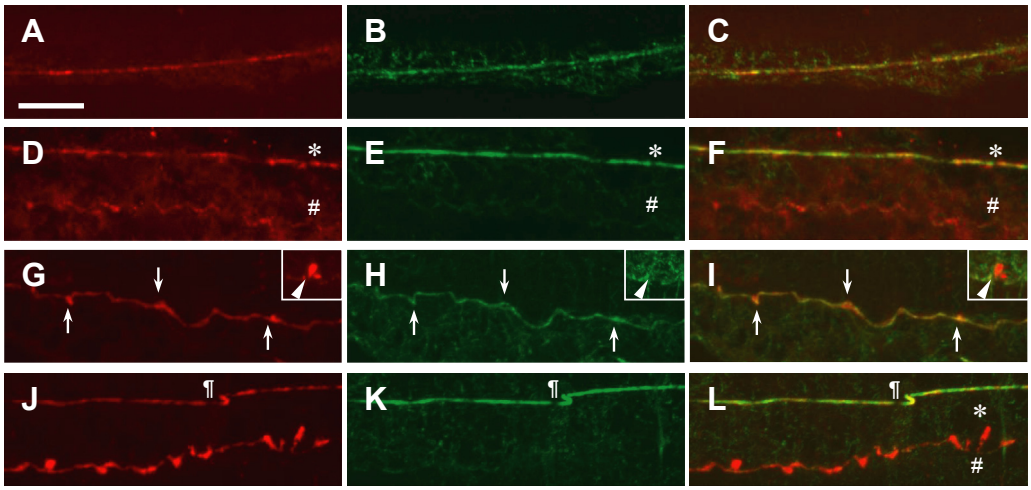

Fig. 6. The localization of tubulin in affected neurites. Paraffin-embedded sections of Mock-Tg (A–C) and R406W(L)-Tg worms (D–L) were colabeled with rabbit anti-DsRed polyclonal (A and D) and DM1A (α-tubulin; B and E), or pool2 (G and J), and DM1A antibodies (H and K). Merged views are shown (C, F, I, and L). The area of tubulin staining is thinner in the affected neurites (#) than in the normal neurites (*). The artifact due to specimen wrinkling is indicated by (¶). Tubulin is absent in abnormally swelling portions associated with kinks (G and H; arrows) and protrusions (arrowheads in inset). Bar = 10 μm. Abbreviation: Tg, transgenic.

Tg and R406W(L)-Tg lines (Fig. 8A and B). The number of protrusions in the same neurites was also significantly decreased by the curcumin treatment (Fig. 8A and C). Taken together, curcumin improves not only neuronal dysfunction but also morphological abnormalities in the tau-Tg worms.

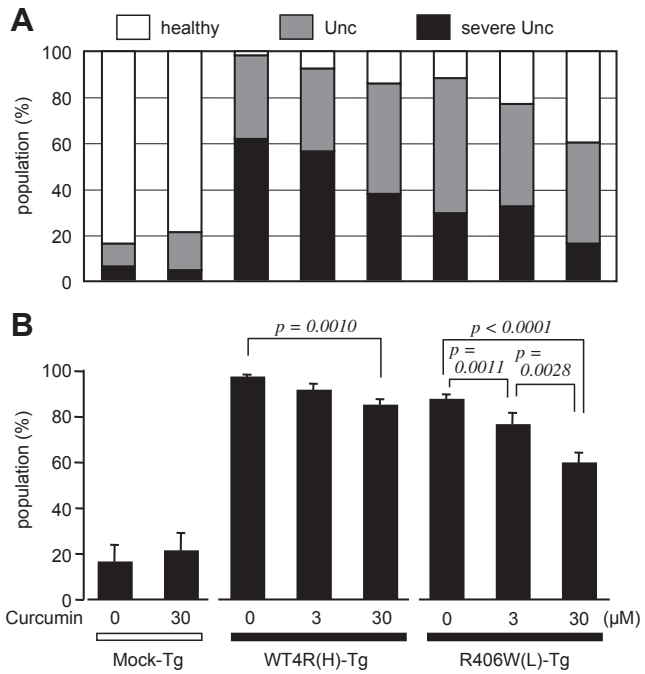

Fig. 7. Curcumin improves behavioral abnormalities in wild-type and mutant tau-expressing worms. (A) Non–tau-Tg, WT4R(H)-Tg, and R406W(L)-Tg worms were grown on NGM plates supplemented with or without curcumin for 3 days and subjected to behavioral analysis. The data show the populations of healthy (open bar), weak Unc (hatched bar), and severe Unc (closed bar) worms (n = 60–100) in each line. (B) The averaged populations (means ± standard error) of total Unc worms from 3 to 5 independent experiments are shown. High doses of curcumin significantly improved the behavioral abnormalities in mutant tau-expressing worms. The statistical significance within each transgenic line was analyzed using the Tukey/Kramer test. Abbreviations: NGM, nematode growth media; Tg, transgenic; Unc, uncoordinated movement.

3.9. Curcumin increased the levels of acetylated α-tubulin

Cumulative lines of evidence indicate that curcumin affects the cytoskeletal organization in neurites. A biochemical analysis of microtubules in the Tg worms was performed. The microtubules and free tubulin in the worms were fractionated, but there was no difference in the amount of microtubule-forming tubulin between the vehicle- and curcumin-treated animals (Fig. 10A). However, the amount of acetylated α-tubulin in the microtubule fraction was significantly increased in the curcumin-treated worms (Fig. 10A and B). As the acetylation of α-tubulin occurs in association with microtubule stabilization, it is possible that curcumin enhances microtubule stability in neurons. Most of the expressed tau that does not bind to microtubules is likely hyperphosphorylated (Fig. 10A). MEC-12, an α-tubulin isoform, can be acetylated and is expressed in the mechanosensory neurons in *C. elegans*, which are involved in the escape response from gentle body touch (Fukushige et al., 1999). To assess whether the acetylation of MEC-12 is associated with neuronal function, touch sensitivity was evaluated in curcumin-treated animals. The WT4R(H)-Tg line displayed abnormalities toward the touch sense that could be discriminated from the Unc phenotype (Fig. 10C). Curcumin treatment improved the dysfunction of the touch neurons, and this improvement could presumably be related to MEC-12 acetylation. These data suggest that curcumin protects neurons from tauopathy via microtubule stabilization.

3.10. Curcumin ameliorated the behavioral abnormalities in tau fragment-expressing worms

Tau fragments that consist of the microtubule-binding domain are highly prone to aggregation (Fatouros et al., 2012; Wang et al., 2009). Consistent with the previous study, the worms expressing C-terminal fragments of 4-repeat tau showed severe behavioral abnormalities and contained dimers that were stable in SDS (Fig. 11; Xie et al., 2014). To determine whether curcumin affected tau oligomer formation, the worms expressing the tau fragments were fed curcumin. High doses of curcumin reduced the population of worms displaying the severe Unc phenotype. However, curcumin did not have an effect on the formation of tau-fragment dimers.

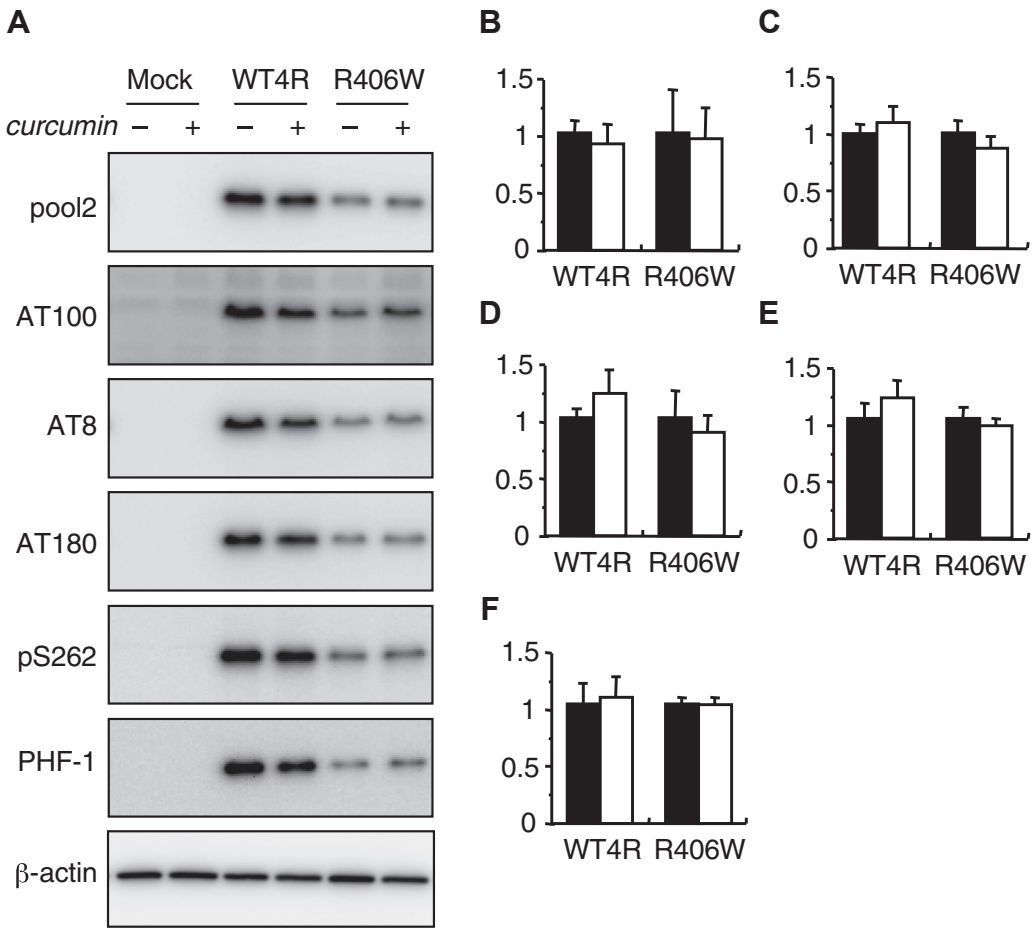

Fig. 8. Curcumin has no effect on tau phosphorylation. (A) Total lysates from non–tau-Tg (Mock), WT4R(H), and R406W(L) lines with or without curcumin treatment were subjected to Western blotting using the indicated antibodies. The band intensities of AT100 (B), AT8 (C), AT180 (D), pS262 (E), and PHF-1 (F) are normalized to total tau (pool2). The statistical analyses were performed using Welch's *t*-test. Abbreviation: Tg, transgenic.

Thus, we conclude that curcumin improves neuronal dysfunction in a manner that is independent of tau aggregation.

4. Discussion

In this study, we developed new lines of tau-expressing *C. elegans* that exhibit behavioral abnormalities in a dose- and mutation-dependent manner. In these models, tau is phosphorylated on many sites similar to those that were identified in PHF-tau. Hyperphosphorylation of tau occurred even in seemingly healthy worms, but none of the lines developed detergent-insoluble aggregates. The behaviorally affected worms were associated with progressive neuritic abnormalities and loss of microtubules accompanied by tau accumulation. We further report that curcumin can suppress both the behavioral and morphological abnormalities. Finally, microtubule stabilization, rather than aggregation inhibition, likely accounts for the beneficial effects of curcumin.

It is unknown how neuronal dysfunction in tauopathy is caused. Previous evidence suggests that the formation of pathological inclusions, such as neurofibrillary tangles, may not necessarily be required for neuronal death but may instead represent a protective measure of the neuron (Berger et al., 2007). Besides our tau-Tg worm models, Spittaels et al. (1999) examined a mouse model overexpressing 4-repeat human tau and found that axonal degeneration was raised without neurofibrillary tangle formation, suggesting that there may be similar mechanisms of tau toxicity in worms and mice. At present, oligomers or small, soluble aggregates of tau are the proposed cause of toxicity, but this assumption remains controversial (Berger et al., 2007; Maeda et al., 2006, 2007; Sahara et al., 2008). Conversely, it has been reported that tau deficiency rescues neuronal dysfunction that is induced by the overexpression of APP (Ittner et al., 2010; Roberson et al., 2007, 2011). This suggests that tau toxicity may be mediated by something other than aggregation. What is known at present is that the propensity for tau aggregation may be linked, presumably in an indirect way, to tau-mediated toxicity.

Even soluble monomeric tau resulted in toxicity in our worm models; however, we cannot completely exclude the possibility of minute levels of soluble toxic oligomers. In the nematode model of tauopathy presented in this study, no insoluble aggregates were found in the affected worms, even at the later stages of life. This is not consistent with a previous model and may be caused by differences in the promoter sequences that were used. Another possible explanation for this difference is that the tau-expression levels were different. We failed to detect conformationally abnormal tau with the MC-1 antibody (data not shown; Jicha et al., 1997). Nevertheless, tau was phosphorylated at the sites identified in PHF-tau, which aggregates in the brains of AD and frontotemporal dementia with parkinsonism-17 patients, and was not bound to microtubules (Miyasaka et al., 2001a, 2001b; Morishima-Kawashima et al., 1995; Yoshida and Ihara, 1993). A panel of anti–phospho-tau specific antibodies was unable to

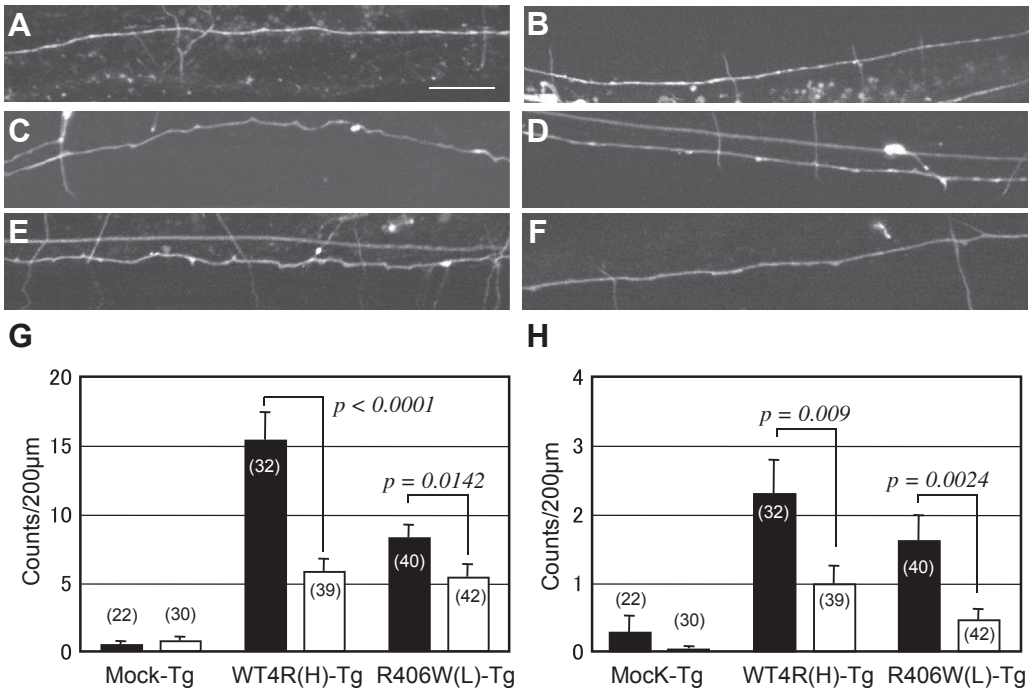

Fig. 9. Curcumin improves neuritic abnormalities in tau-expressing worms. (A) The fluorescence of DsRed expressed in the neurons of Mock-Tg worm (A and B), WT4R(H)-Tg (C and D), and R406W(L)-Tg (E and F) without (A, C, and E) or with 30 μM of curcumin treatment (B, D, and F) for 10 days are shown. Abnormal kinks (G) and protrusions (H) in vehicle- (closed bar) or curcumin- (open bar) treated animals were quantified. The data represent the mean counts of kinks and protrusions along 200 μm of the affected neurites ± standard error (n = 22–43 animals). The statistical significance between vehicle- and curcumin-treated animals within each Tg line were analyzed using Welch's *t*-test. Abbreviation: Tg, transgenic.

identify specific phosphorylation sites that were only found in the affected worms. Thus, hyperphosphorylation may not be sufficient for tau aggregation. We previously reported that tau is liberated from the microtubules and subsequently hyperphosphorylated (Miyasaka et al., 2010). Taken together, it is possible that the microtubule-unbound tau, which is susceptible to phosphorylation, could trigger neuronal dysfunction in tauopathy.

Neuritic abnormalities consist of loss of tubulin (microtubules), and tau accumulation (Cash et al., 2003; Gray et al., 1987; Paula-Barbosa et al., 1987). Other *C. elegans* models and various in vivo models of tauopathy also share these characteristics (Miyasaka et al., 2005a; Tatebayashi et al., 2002). Previously, it has been reported that acute tau phosphorylation does not induce microtubule destruction (Planel et al., 2008). Conversely, microtubule destruction induces tau liberation and the subsequent phosphorylation (Miyasaka et al., 2010). Thus, massive microtubule degeneration may occur in the comparatively early stage of the cascade of tauopathy. Related to this, it would be reasonable to postulate that the formation of detergent-insoluble aggregate of tau occurs in the late stage of soluble tau accumulation.

Although various mammalian models have provided important insight into the detailed mechanisms of tauopathy, it is not possible to use these models for large-scale drug screening. In contrast, invertebrate models can be used for the rapid screening of small compounds. *C. elegans* is widely used for basic biological studies, especially large scale genetic screens for behavioral and morphological abnormalities (Fraser et al., 2000). This characteristic prompted us to use this model to screen drugs that would treat neurodegenerative diseases. In this study, we were able to evaluate the anti-tauopathy effect of various compounds within a few days. This may be the shortest time period for in vivo analyses and suggests the feasibility of this model for strategic drug screening. Using this in vivo model provides an opportunity to discover new candidate compounds that are involved in as-yet unidentified steps to the tau-induced neuronal dysfunction. This unbiased system may also provide new insights into the disease mechanism as well as new drug targets against tauopathy.

One important question is whether a compound that is effective in the worm model is also effective in the mouse model. If so, the disease mechanism may be the same in both species. In particular, we believe that a mechanism other than aggregate formation may cause tauopathy. Curcumin was administered to P301L mice from 20 to 23 months of age. Preliminary observations indicate that curcumin reduces the number of tau-accumulated neurons and improves the neuritic abnormalities in the brain (article in preparation). Ma et al. (2013) also reported that the curcumin reduced soluble tau and behavioral abnormalities in tau-Tg mice, possibly through the elevation of heat shock proteins. Although there are various views on the mechanism, curcumin is effective in treating tauopathy in several preclinical models.

There are limitations with the worm models; compounds that do not penetrate the cuticle are excluded from the screening. However, the mutants of acs-20 and acs-22 genes that are defective in the cuticle barrier could allow for the penetration of small molecules into the worms (Kage-Nakadai et al., 2010). The application of these mutants as disease models would be highly promising to extend the use of the *C. elegans* model for drug screening. The benefits of this model system over other models, such as easy handling and rapid screening, are significant.

We note that trehalose, which is an inducer of autophagy and a chemical chaperon had no protective effects on our tau-Tg worms. These results may be explained by the lack of insoluble aggregations in the tau-Tg worms. Also, the lower dose used here may be another reason for the negative results. As a suppressor of nematode aging, over 100-fold higher trehalose doses were used in a previous study (Honda et al., 2010).

Curcumin improves tau-induced neuronal dysfunction and neuritic abnormalities in the *C. elegans* model of tauopathy. This

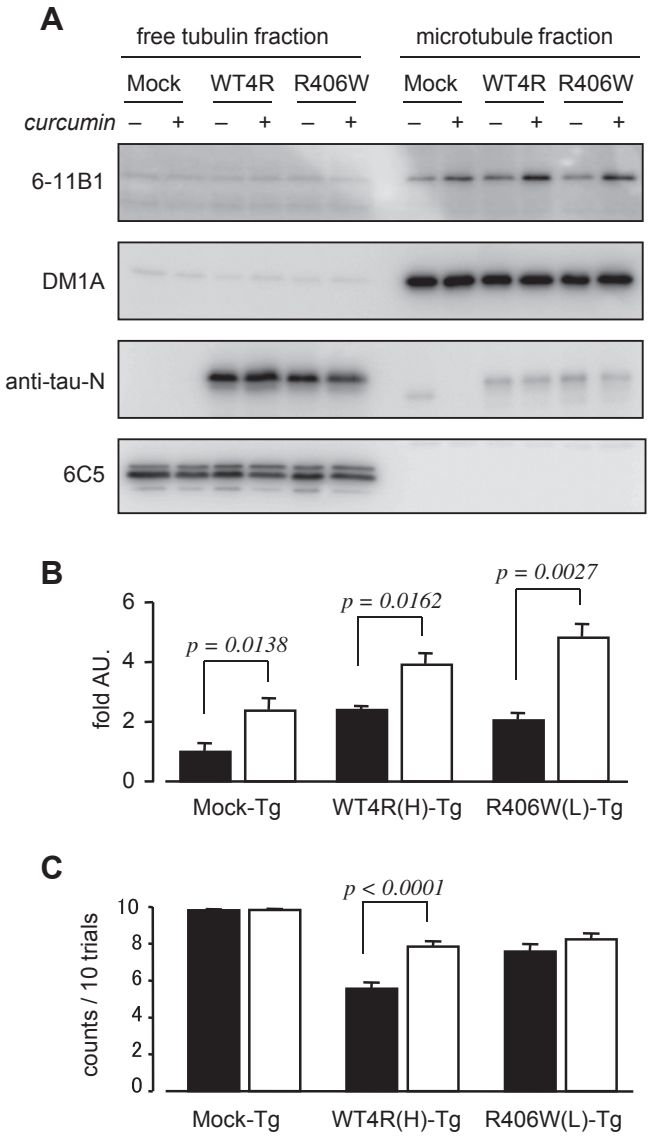

Fig. 10. Curcumin increased the levels of acetylated α-tubulin. (A) Free tubulin and microtubule fractions were prepared from vehicle- or curcumin- (30 μM) treated Mock-Tg (Mock), WT4R(H)-Tg, and R406 W(L)-Tg worms. Equal amounts of proteins were subjected to western blotting using antibodies against acetylated α-tubulin (6–11B1), total α-tubulin (DM1A), tau (anti–tau-N), and GAPDH (6C5). (B) Relative amounts of acetylated tubulin in vehicle- (closed bar) or curcumin- (open bar) treated animals were quantified. The data represent the means of 3 independent experiments. (C) Touch sense abnormalities in the tau-expressing worms were improved by the curcumin treatment. Vehicle- (closed bar) and curcumin- (open bar) treated animals were subjected to the touch assay. The data represent the means of the counts of normal touch responses in 10 trials (5 for the anterior plus 5 for the posterior, n = 60–80). Statistical significance between vehicle- and curcumin-treated animals in each line was analyzed using the Tukey/Kramer test. Abbreviations: GAPDH, glyceraldehyde-3-phosphate dehydrogenase; Tg, transgenic.

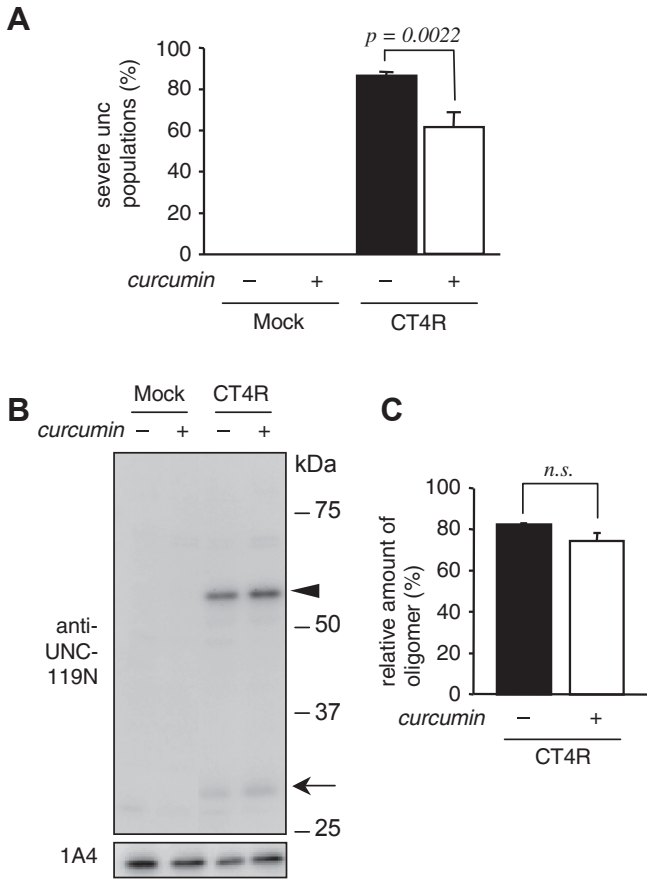

Fig. 11. Curcumin improved behavioral abnormalities, but it did not affect tau dimer formation. (A and B) C-terminal fragment-expressing worms (CT4R-Tg) were treated with the vehicle or curcumin (100 μM) for 3 days and subjected to (A) behavioral analysis and (B) Western blotting using anti–UNC-119N and α-actin antibodies (1A4). Tau fragment monomers (arrow) and dimers (arrowhead) are shown. (C) The relative amounts of the dimers were quantified. The means of 3 independent experiments are shown. Statistical significance was analyzed using Student's *t* test. Abbreviation: Tg, transgenic.

indicates that curcumin is a strong candidate for an anti-tauopathy drug. Curcumin is already known to suppress Aβ aggregation, and its effectiveness was confirmed using Tg mouse models, although recently conducted phase II trials in patients with mild cognitive impairment and AD were reported to have failed. This failure may be partially due to low bioavailability (Ringman et al., 2012). In this study, we show that curcumin is also effective to treat tauopathy. Surprisingly, curcumin did not suppress tau phosphorylation or aggregation, but it did protect the worms from neuritic and cytoskeletal abnormalities. Although the pharmacological targets of curcumin are not identified, increased levels of acetylated α-tubulin suggest that microtubule stabilization is involved, either directly or indirectly. Kraemer et al. (2006) reported many genetic modifiers of Unc movement in a tau-Tg worm model, including chaperones, phosphatases, and kinases, some of which may influence microtubule stabilization, raising several possible candidate targets of curcumin. Curcumin has been reported to induce Skn-1/Nrf2 pathway, which has a crucial role in maintaining cellular redox homeostasis. (Jimenez-Osorio et al., 2015). Thus, it is possible that the skn-1/Nrf2 pathway was involved in the anti-tauopathy effect of curcumin, because the Nrf2 activation presumably rescued tauopathy in mouse model (Stack et al., 2014). It can be considered that the unidentified factors underlying skn-1/Nrf2 pathway may have a potential to protect the neurodegeneration due to tauopathy through the stabilization of microtubules.

Microtubule destruction is the central event that occurs in neurons affected by tau and should be targeted to treat tauopathy. Recent reports indicate that microtubule stabilizers can improve tauopathy, which is consistent with the effectiveness of curcumin in tau-Tg worms (Barten et al., 2012; Brunden et al., 2010, 2012; Matsuoka et al., 2007, 2008; Shiryaev et al., 2009; Zhang et al., 2012). A recent study showing that curcumin extends the lifespan of *C. elegans* by maintaining protein homeostasis strongly supports the view that curcumin stabilizes tubulin or microtubules in

neurons (Alavez et al., 2011). We are currently trying at the screening of curcumin derivatives that have enhanced bioavailability and stabilize microtubules and are effective against tauopathy.

Disclosure statement

The authors report no conflict of interest.

Acknowledgements

This work was supported in part by a Grant-in-Aid for Exploratory Research (22650074 to Tomohiro Miyasaka), Core Research for Evolutional Science and Technology (to Yasuo Ihara) by the Japan Science and Technology Agency (JST), and "Integrated research on neuropsychiatric disorder" carried out under the Strategic Research Program for Brain Sciences (to Tomohiro Miyasaka and Yasuo Ihara) from Japan Agency for Medical Research and development (AMED), Japan. The authors thank Akiko Saka for technical assistance in the development of the worms used in this study.

Appendix A. Supplementary data

Supplementary data associated with this article can be found, in the online version, at http://dx.doi.org/10.1016/j.neurobiolaging.2015.11.004.

References

Aamodt, E.J., Culotti, J.G., 1986. Microtubules and microtubule-associated proteins from the nematode Caenorhabditis elegans: periodic cross-links connect microtubules in vitro. J. Cell Biol. 103, 23–31.
Alavez, S., Vantipalli, M.C., Zucker, D.J., Klang, I.M., Lithgow, G.J., 2011. Amyloid-binding compounds maintain protein homeostasis during ageing and extend lifespan. Nature 472, 226–229.
Aoyagi, H., Hasegawa, M., Tamaoka, A., 2007. Fibrillogenic nuclei composed of P301L mutant tau induce elongation of P301L tau but not wild-type tau. J. Biol. Chem. 282, 20309–20318.
Barten, D.M., Fanara, P., Andorfer, C., Hoque, N., Wong, P.Y., Husted, K.H., Cadelina, G.W., Decarr, L.B., Yang, L., Liu, V., Fessler, C., Protassio, J., Riff, T., Turner, H., Janus, C.G., Sankaranarayanan, S., Polson, C., Meredith, J.E., Gray, G., Hanna, A., Olson, R.E., Kim, S.H., Vite, G.D., Lee, F.Y., Albright, C.F., 2012. Hyperdynamic microtubules, cognitive deficits, and pathology are improved in tau transgenic mice with low doses of the microtubule-stabilizing agent BMS-241027. J. Neurosci. 32, 7137–7145.
Begum, A.N., Jones, M.R., Lim, G.P., Morihara, T., Kim, P., Heath, D.D., Rock, C.L., Pruitt, M.A., Yang, F., Hudspeth, B., Hu, S., Faull, K.F., Teter, B., Cole, G.M., Frautschy, S.A., 2008. Curcumin structure-function, bioavailability, and efficacy in models of neuroinflammation and Alzheimer's disease. J. Pharmacol. Exp. Ther. 326, 196–208.
Belkacemi, A., Doggui, S., Dao, L., Ramassamy, C., 2011. Challenges associated with curcumin therapy in Alzheimer disease. Expert Rev. Mol. Med. 13, e34.
Berger, Z., Roder, H., Hanna, A., Carlson, A., Rangachari, V., Yue, M., Wszolek, Z., Ashe, K., Knight, J., Dickson, D., Andorfer, C., Rosenberry, T.L., Lewis, J., Hutton, M., Janus, C., 2007. Accumulation of pathological tau species and memory loss in a conditional model of tauopathy. J. Neurosci. 27, 3650–3662.
Boutajangout, A., Sigurdsson, E.M., Krishnamurthy, P.K., 2011. Tau as a therapeutic target for Alzheimer's disease. Curr. Alzheimer Res. 8, 666–677.
Braak, H., Braak, E., 1997. Frequency of stages of Alzheimer-related lesions in different age categories. Neurobiol. Aging 18, 351–357.
Brenner, S., 1974. The genetics of Caenorhabditis elegans. Genetics 77, 71–94.
Brunden, K.R., Ballatore, C., Lee, V.M., Smith 3rd, A.B., Trojanowski, J.Q., 2012. Brain-penetrant microtubule-stabilizing compounds as potential therapeutic agents for tauopathies. Biochem. Soc. Trans. 40, 661–666.
Brunden, K.R., Zhang, B., Carroll, J., Yao, Y., Potuzak, J.S., Hogan, A.M., Iba, M., James, M.J., Xie, S.X., Ballatore, C., Smith 3rd, A.B., Lee, V.M., Trojanowski, J.Q., 2010. Epothilone D improves microtubule density, axonal integrity, and cognition in a transgenic mouse model of tauopathy. J. Neurosci. 30, 13861–13866.
Cash, A.D., Aliev, G., Siedlak, S.L., Nunomura, A., Fujioka, H., Zhu, X., Raina, A.K., Vinters, H.V., Tabaton, M., Johnson, A.B., Paula-Barbosa, M., Avila, J., Jones, P.K., Castellani, R.J., Smith, M.A., Perry, G., 2003. Microtubule reduction in Alzheimer's disease and aging is independent of tau filament formation. Am. J. Pathol. 162, 1623–1627.
Chandra, V., Pandav, R., Dodge, H.H., Johnston, J.M., Belle, S.H., DeKosky, S.T., Ganguli, M., 2001. Incidence of Alzheimer's disease in a rural community in India: the Indo-US study. Neurology 57, 985–989.
Corbett, A., Smith, J., Ballard, C., 2012. New and emerging treatments for Alzheimer's disease. Expert Rev. Neurother. 12, 535–543.
Delacourte, A., David, J.P., Sergeant, N., Buee, L., Wattez, A., Vermersch, P., Ghozali, F., Fallet-Bianco, C., Pasquier, F., Lebert, F., Petit, H., Di Menza, C., 1999. The biochemical pathway of neurofibrillary degeneration in aging and Alzheimer's disease. Neurology 52, 1158–1165.
Fatouros, C., Pir, G.J., Biernat, J., Koushika, S.P., Mandelkow, E., Mandelkow, E.M., Schmidt, E., Baumeister, R., 2012. Inhibition of tau aggregation in a novel Caenorhabditis elegans model of tauopathy mitigates proteotoxicity. Hum. Mol. Genet. 21, 3587–3603.
Fraser, A.G., Kamath, R.S., Zipperlen, P., Martinez-Campos, M., Sohrmann, M., Ahringer, J., 2000. Functional genomic analysis of C. elegans chromosome I by systematic RNA interference. Nature 408, 325–330.
Fukushige, T., Siddiqui, Z.K., Chou, M., Culotti, J.G., Gogonea, C.B., Siddiqui, S.S., Hamelin, M., 1999. MEC-12, an alpha-tubulin required for touch sensitivity in C. elegans. J. Cell Sci 112 (Pt 3), 395–403.
Goate, A., Hardy, J., 2012. Twenty years of Alzheimer's disease-causing mutations. J. Neurochem. 120 (Suppl 1), 3–8.
Gomez-Isla, T., Hollister, R., West, H., Mui, S., Growdon, J.H., Petersen, R.C., Parisi, J.E., Hyman, B.T., 1997. Neuronal loss correlates with but exceeds neurofibrillary tangles in Alzheimer's disease. Ann. Neurol. 41, 17–24.
Gotz, J., Chen, F., van Dorpe, J., Nitsch, R.M., 2001. Formation of neurofibrillary tangles in P301l tau transgenic mice induced by Abeta 42 fibrils. Science 293, 1491–1495.
Gray, E.G., Paula-Barbosa, M., Roher, A., 1987. Alzheimer's disease: paired helical filaments and cytomembranes. Neuropathol. Appl. Neurobiol. 13, 91–110.
Hasegawa, M., Morishima-Kawashima, M., Takio, K., Suzuki, M., Titani, K., Ihara, Y., 1992. Protein sequence and mass spectrometric analyses of tau in the Alzheimer's disease brain. J. Biol. Chem. 267, 17047–17054.
Holmes, C., Boche, D., Wilkinson, D., Yadegarfar, G., Hopkins, V., Bayer, A., Jones, R.W., Bullock, R., Love, S., Neal, J.W., Zotova, E., Nicoll, J.A., 2008. Long-term effects of Abeta42 immunisation in Alzheimer's disease: follow-up of a randomised, placebo-controlled phase I trial. Lancet 372, 216–223.
Honda, Y., Tanaka, M., Honda, S., 2010. Trehalose extends longevity in the nematode Caenorhabditis elegans. Aging Cell 9, 558–569.
Ittner, L.M., Ke, Y.D., Delerue, F., Bi, M., Gladbach, A., van Eersel, J., Wolfing, H., Chieng, B.C., Christie, M.J., Napier, I.A., Eckert, A., Staufenbiel, M., Hardeman, E., Gotz, J., 2010. Dendritic function of tau mediates amyloid-beta toxicity in Alzheimer's disease mouse models. Cell 142, 387–397.
Jicha, G.A., Bowser, R., Kazam, I.G., Davies, P., 1997. Alz-50 and MC-1, a new monoclonal antibody raised to paired helical filaments, recognize conformational epitopes on recombinant tau. J. Neurosci. Res. 48, 128–132.
Jimenez-Osorio, A.S., Gonzalez-Reyes, S., Pedraza-Chaverri, J., 2015. Natural Nrf2 activators in diabetes. Clin. Chim. Acta 448, 182–192.
Kage-Nakadai, E., Kobuna, H., Kimura, M., Gengyo-Ando, K., Inoue, T., Arai, H., Mitani, S., 2010. Two very long chain fatty acid acyl-CoA synthetase genes, acs-20 and acs-22, have roles in the cuticle surface barrier in Caenorhabditis elegans. PloS One 5, e8857.
Kraemer, B.C., Burgess, J.K., Chen, J.H., Thomas, J.H., Schellenberg, G.D., 2006. Molecular pathways that influence human tau-induced pathology in Caenorhabditis elegans. Hum. Mol. Genet. 15, 1483–1496.
Kraemer, B.C., Zhang, B., Leverenz, J.B., Thomas, J.H., Trojanowski, J.Q., Schellenberg, G.D., 2003. Neurodegeneration and defective neurotransmission in a Caenorhabditis elegans model of tauopathy. Proc. Natl. Acad. Sci. U. S. A. 100, 9980–9985.
Lee, V.M., Goedert, M., Trojanowski, J.Q., 2001. Neurodegenerative tauopathies. Annu. Rev. Neurosci. 24, 1121–1159.
Lewis, J., Dickson, D.W., Lin, W.L., Chisholm, L., Corral, A., Jones, G., Yen, S.H., Sahara, N., Skipper, L., Yager, D., Eckman, C., Hardy, J., Hutton, M., McGowan, E., 2001. Enhanced neurofibrillary degeneration in transgenic mice expressing mutant tau and APP. Science 293, 1487–1491.
Lim, G.P., Chu, T., Yang, F., Beech, W., Frautschy, S.A., Cole, G.M., 2001. The curry spice curcumin reduces oxidative damage and amyloid pathology in an Alzheimer transgenic mouse. J. Neurosci. 21, 8370–8377.
Ma, Q.L., Yang, F., Rosario, E.R., Ubeda, O.J., Beech, W., Gant, D.J., Chen, P.P., Hudspeth, B., Chen, C., Zhao, Y., Vinters, H.V., Frautschy, S.A., Cole, G.M., 2009. Beta-amyloid oligomers induce phosphorylation of tau and inactivation of insulin receptor substrate via c-Jun N-terminal kinase signaling: suppression by omega-3 fatty acids and curcumin. J. Neurosci. 29, 9078–9089.
Ma, Q.L., Zuo, X., Yang, F., Ubeda, O.J., Gant, D.J., Alaverdyan, M., Teng, E., Hu, S., Chen, P.P., Maiti, P., Teter, B., Cole, G.M., Frautschy, S.A., 2013. Curcumin suppresses soluble tau dimers and corrects molecular chaperone, synaptic, and behavioral deficits in aged human tau transgenic mice. J. Biol. Chem. 288, 4056–4065.
Maduro, M., Pilgrim, D., 1995. Identification and cloning of unc-119, a gene expressed in the Caenorhabditis elegans nervous system. Genetics 141, 977–988.
Maeda, S., Sahara, N., Saito, Y., Murayama, M., Yoshiike, Y., Kim, H., Miyasaka, T., Murayama, S., Ikai, A., Takashima, A., 2007. Granular tau oligomers as intermediates of tau filaments. Biochemistry 46, 3856–3861.

Maeda, S., Sahara, N., Saito, Y., Murayama, S., Ikai, A., Takashima, A., 2006. Increased levels of granular tau oligomers: an early sign of brain aging and Alzheimer's disease. Neurosci. Res. 54, 197–201.
Mangialasche, F., Solomon, A., Winblad, B., Mecocci, P., Kivipelto, M., 2010. Alzheimer's disease: clinical trials and drug development. Lancet Neurol. 9, 702–716.
Matsuoka, Y., Gray, A.J., Hirata-Fukae, C., Minami, S.S., Waterhouse, E.G., Mattson, M.P., LaFerla, F.M., Gozes, I., Aisen, P.S., 2007. Intranasal NAP administration reduces accumulation of amyloid peptide and tau hyperphosphorylation in a transgenic mouse model of Alzheimer's disease at early pathological stage. J. Mol. Neurosci. 31, 165–170.
Matsuoka, Y., Jouroukhin, Y., Gray, A.J., Ma, L., Hirata-Fukae, C., Li, H.F., Feng, L., Lecanu, L., Walker, B.R., Planel, E., Arancio, O., Gozes, I., Aisen, P.S., 2008. A neuronal microtubule-interacting agent, NAPVSIPQ, reduces tau pathology and enhances cognitive function in a mouse model of Alzheimer's disease. J. Pharmacol. Exp. Ther. 325, 146–153.
Mayeux, R., Stern, Y., 2012. Epidemiology of Alzheimer disease. Cold Spring Harb. Perspect. Med. 2.
Mello, C., Fire, A., 1995. DNA transformation. Methods Cell Biol. 48, 451–482.
Mello, C.C., Kramer, J.M., Stinchcomb, D., Ambros, V., 1991. Efficient gene transfer in C.elegans: extrachromosomal maintenance and integration of transforming sequences. EMBO J. 10, 3959–3970.
Mitani, S., 1995. Genetic regulation of mec-3 gene expression implicated in the specification of the mechanosensory neuron cell types in Caenorhabditis elegans. Dev. Growth Differ. 37, 551–557.
Miyasaka, T., Ding, Z., Gengyo-Ando, K., Oue, M., Yamaguchi, H., Mitani, S., Ihara, Y., 2005a. Progressive neurodegeneration in C. elegans model of tauopathy. Neurobiol. Dis. 20, 372–383.
Miyasaka, T., Morishima-Kawashima, M., Ravid, R., Heutink, P., van Swieten, J.C., Nagashima, K., Ihara, Y., 2001a. Molecular analysis of mutant and wild-type tau deposited in the brain affected by the FTDP-17 R406W mutation. Am. J. Pathol. 158, 373–379.
Miyasaka, T., Morishima-Kawashima, M., Ravid, R., Kamphorst, W., Nagashima, K., Ihara, Y., 2001b. Selective deposition of mutant tau in the FTDP-17 brain affected by the P301L mutation. J. Neuropathol. Exp. Neurol. 60, 872–884.
Miyasaka, T., Sato, S., Tatebayashi, Y., Takashima, A., 2010. Microtubule destruction induces tau liberation and its subsequent phosphorylation. FEBS Lett. 584, 3227–3232.
Miyasaka, T., Watanabe, A., Saito, Y., Murayama, S., Mann, D.M., Yamazaki, M., Ravid, R., Morishima-Kawashima, M., Nagashima, K., Ihara, Y., 2005b. Visualization of newly deposited tau in neurofibrillary tangles and neuropil threads. J. Neuropathol. Exp. Neurol. 64, 665–674.
Morishima-Kawashima, M., Hasegawa, M., Takio, K., Suzuki, M., Yoshida, H., Watanabe, A., Titani, K., Ihara, Y., 1995. Hyperphosphorylation of tau in PHF. Neurobiol. Aging 16, 365–371 discussion 71–80.
Ono, K., Hasegawa, K., Naiki, H., Yamada, M., 2004. Curcumin has potent anti-amyloidogenic effects for Alzheimer's beta-amyloid fibrils in vitro. J. Neurosci. Res. 75, 742–750.
Paula-Barbosa, M., Tavares, M.A., Cadete-Leite, A., 1987. A quantitative study of frontal cortex dendritic microtubules in patients with Alzheimer's disease. Brain Res. 417, 139–142.
Planel, E., Krishnamurthy, P., Miyasaka, T., Liu, L., Herman, M., Kumar, A., Bretteville, A., Figueroa, H.Y., Yu, W.H., Whittington, R.A., Davies, P., Takashima, A., Nixon, R.A., Duff, K.E., 2008. Anesthesia-induced hyperphosphorylation detaches 3-repeat tau from microtubules without affecting their stability in vivo. J. Neurosci. 28, 12798–12807.
Ringman, J.M., Frautschy, S.A., Teng, E., Begum, A.N., Bardens, J., Beigi, M., Gylys, K., Badmaev, V., Heath, D., Apostolova, L.G., Porter, V., Vanek, Z., Marshall, G.A., Hellemann, G., Sugar, C., Masterman, D., Montine, T.J., Cummings, J.L., Cole, G.M., 2012. Oral curcumin for Alzheimer's disease: tolerability and efficacy in a 24-week randomized, double blind, placebo-controlled study. Alzheimers Res. Ther. 4, 43.
Roberson, E.D., Halabisky, B., Yoo, J.W., Yao, J., Chin, J., Yan, F., Wu, T., Hamto, P., Devidze, N., Yu, G.Q., Palop, J.J., Noebels, J.L., Mucke, L., 2011. Amyloid-beta/Fyn-induced synaptic, network, and cognitive impairments depend on tau levels in multiple mouse models of Alzheimer's disease. J. Neurosci. 31, 700–711.
Roberson, E.D., Scearce-Levie, K., Palop, J.J., Yan, F., Cheng, I.H., Wu, T., Gerstein, H., Yu, G.Q., Mucke, L., 2007. Reducing endogenous tau ameliorates amyloid beta-induced deficits in an Alzheimer's disease mouse model. Science 316, 750–754.
Sahara, N., Maeda, S., Takashima, A., 2008. Tau oligomerization: a role for tau aggregation intermediates linked to neurodegeneration. Curr. Alzheimer Res. 5, 591–598.
Santacruz, K., Lewis, J., Spires, T., Paulson, J., Kotilinek, L., Ingelsson, M., Guimaraes, A., DeTure, M., Ramsden, M., McGowan, E., Forster, C., Yue, M., Orne, J., Janus, C., Mariash, A., Kuskowski, M., Hyman, B., Hutton, M., Ashe, K.H., 2005. Tau suppression in a neurodegenerative mouse model improves memory function. Science 309, 476–481.
Selkoe, D.J., 2012. Preventing Alzheimer's disease. Science 337, 1488–1492.
Shiryaev, N., Jouroukhin, Y., Giladi, E., Polyzoidou, E., Grigoriadis, N.C., Rosenmann, H., Gozes, I., 2009. NAP protects memory, increases soluble tau and reduces tau hyperphosphorylation in a tauopathy model. Neurobiol. Dis. 34, 381–388.
Spittaels, K., Van den Haute, C., Van Dorpe, J., Bruynseels, K., Vandezande, K., Laenen, I., Geerts, H., Mercken, M., Sciot, R., Van Lommel, A., Loos, R., Van Leuven, F., 1999. Prominent axonopathy in the brain and spinal cord of transgenic mice over-expressing four-repeat human tau protein. Am. J. Pathol. 155, 2153–2165.
Stack, C., Jainuddin, S., Elipenahli, C., Gerges, M., Starkova, N., Starkov, A.A., Jove, M., Portero-Otin, M., Launay, N., Pujol, A., Kaidery, N.A., Thomas, B., Tampellini, D., Beal, M.F., Dumont, M., 2014. Methylene blue upregulates Nrf2/ARE genes and prevents tau-related neurotoxicity. Hum. Mol. Genet. 23, 3716–3732.
Tanaka, M., Machida, Y., Niu, S., Ikeda, T., Jana, N.R., Doi, H., Kurosawa, M., Nekooki, M., Nukina, N., 2004. Trehalose alleviates polyglutamine-mediated pathology in a mouse model of Huntington disease. Nat. Med. 10, 148–154.
Tank, E.M., Rodgers, K.E., Kenyon, C., 2011. Spontaneous age-related neurite branching in Caenorhabditis elegans. J. Neurosci. 31, 9279–9288.
Tatebayashi, Y., Miyasaka, T., Chui, D.H., Akagi, T., Mishima, K., Iwasaki, K., Fujiwara, M., Tanemura, K., Murayama, M., Ishiguro, K., Planel, E., Sato, S., Hashikawa, T., Takashima, A., 2002. Tau filament formation and associative memory deficit in aged mice expressing mutant (R406W) human tau. Proc. Natl. Acad. Sci. U. S. A. 99, 13896–13901.
Toth, M.L., Melentijevic, I., Shah, L., Bhatia, A., Lu, K., Talwar, A., Naji, H., Ibanez-Ventoso, C., Ghose, P., Jevince, A., Xue, J., Herndon, L.A., Bhanot, G., Rongo, C., Hall, D.H., Driscoll, M., 2012. Neurite sprouting and synapse deterioration in the aging Caenorhabditis elegans nervous system. J. Neurosci. 32, 8778–8790.
Wang, J., Ho, L., Zhao, Z., Seror, I., Humala, N., Dickstein, D.L., Thiyagarajan, M., Percival, S.S., Talcott, S.T., Pasinetti, G.M., 2006. Moderate consumption of Cabernet Sauvignon attenuates Abeta neuropathology in a mouse model of Alzheimer's disease. FASEB J. 20, 2313–2320.
Wang, Y., Martinez-Vicente, M., Kruger, U., Kaushik, S., Wong, E., Mandelkow, E.M., Cuervo, A.M., Mandelkow, E., 2009. Tau fragmentation, aggregation and clearance: the dual role of lysosomal processing. Hum. Mol. Genet. 18, 4153–4170.
Way, J.C., Chalfie, M., 1988. mec-3, a homeobox-containing gene that specifies differentiation of the touch receptor neurons in C. elegans. Cell 54, 5–16.
Wischik, C., Staff, R., 2009. Challenges in the conduct of disease-modifying trials in AD: practical experience from a phase 2 trial of Tau-aggregation inhibitor therapy. J. Nutr. Health Aging 13, 367–369.
Wischik, C.M., Edwards, P.C., Lai, R.Y., Roth, M., Harrington, C.R., 1996. Selective inhibition of Alzheimer disease-like tau aggregation by phenothiazines. Proc. Natl. Acad. Sci. U. S. A. 93, 11213–11218.
Xie, C., Miyasaka, T., Yoshimura, S., Hatsuta, H., Yoshina, S., Kage-Nakadai, E., Mitani, S., Murayama, S., Ihara, Y., 2014. The homologous carboxyl-terminal domains of microtubule-associated protein 2 and TAU induce neuronal dysfunction and have differential fates in the evolution of neurofibrillary tangles. PloS One 9, e89796.
Yang, F., Lim, G.P., Begum, A.N., Ubeda, O.J., Simmons, M.R., Ambegaokar, S.S., Chen, P.P., Kayed, R., Glabe, C.G., Frautschy, S.A., Cole, G.M., 2005. Curcumin inhibits formation of amyloid beta oligomers and fibrils, binds plaques, and reduces amyloid in vivo. J. Biol. Chem. 280, 5892–5901.
Yoshida, H., Ihara, Y., 1993. Tau in paired helical filaments is functionally distinct from fetal tau: assembly incompetence of paired helical filament-tau. J. Neurochem. 61, 1183–1186.
Zhang, B., Carroll, J., Trojanowski, J.Q., Yao, Y., Iba, M., Potuzak, J.S., Hogan, A.M., Xie, S.X., Ballatore, C., Smith 3rd, A.B., Lee, V.M., Brunden, K.R., 2012. The microtubule-stabilizing agent, epothilone D, reduces axonal dysfunction, neurotoxicity, cognitive deficits, and Alzheimer-like pathology in an interventional study with aged tau transgenic mice. J. Neurosci. 32, 3601–3611.